

# Total Ionizing Dose Effects on Aluminum Oxide/ Zirconium-Doped Hafnium Oxide Stack Ferroelectric Tunneling Junctions

Xueqin Yang<sup>1,2</sup>, Yannan Xu<sup>1,2</sup>, Jinshun Bi<sup>1,2\*</sup>, Kai Xi<sup>1</sup>, Linjie Fan<sup>1,2</sup>, Lanlong Ji<sup>1</sup> & Gaobo Xu<sup>1</sup>

<sup>1</sup>The Institute of Microelectronics of Chinese Academy of Sciences, Beijing 100029, China ;  
<sup>2</sup>The University of Chinese Academy of Sciences, Beijing 100049, China

## Appendix A Importance

*Experiment.* The device was fabricated on a heavily p-doped Ge wafer with the resistivity of 0.003  $\Omega$ -cm. The 2 nm- $\text{Al}_2\text{O}_3$ /10 nm-HZO stack layers were deposited on the Ge substrate by atomic layer deposition (ALD) at 300 °C. The top electrode TiN with the thickness of 40 nm was deposited by an ion-beam sputtering and was patterned. The area of the top electrode was  $10^{-4}$   $\text{cm}^2$  ( $100\mu\text{m}\times 100\mu\text{m}$ ). Finally, rapid thermal annealing (RTA) was carried out to crystallize HZO film at 500 °C for 30 s in  $\text{N}_2$  ambient environment. The structure and the fabrication process of the device are shown in Fig. 1(a). The crystal structure of the ferroelectric layer HZO is analyzed by the grazing incidence X-ray diffraction (GIXRD), while the crystallization and morphology are observed by the high-resolution transmission electron microscopy (HRTEM). The HRTEM images of TiN/HZO/ $\text{Al}_2\text{O}_3$ /P<sup>+</sup>-Ge are shown in Fig. 1(b). The interfaces can be clearly observed, and the ferroelectric layer HZO is mostly polycrystalline. The diffraction peak at 30.57 ° in Fig. 1(c) is considered to be the evidence of the existence of the orthorhombic phase [1].

The unpackaged devices were radiated by the <sup>60</sup>Co  $\gamma$  rays with a radiation rate of 50 rad (Si)/s at Beijing Normal University. The <sup>60</sup>Co  $\gamma$  rays incident vertically on the surface of the samples. After being radiated to a certain dose, the current-voltage (I-V), the capacitance-voltage (C-V), and the write/read operations were measured using Agilent B1500A. In C-V measurement, the AC bias frequency was 1 MHz, and the amplitude was 30 mV. The polarization-voltage hysteresis loop (P-V) and endurance performance were characterized by Radiant Technology Precisions Workstations.

*Results and discussion.* In this device, the switching characteristics are mainly determined by the change of the effective barrier height of  $\text{Al}_2\text{O}_3$ . Specifically, the F-N tunneling dominates at high read voltages, while the polarization after programming or erasing in HZO can modify the effective tunneling barrier height in  $\text{Al}_2\text{O}_3$ , as shown in Figs. 1(d) and (e), so that the tunneling current and resistance are tuned [2]. The read current after erasing decreases after TID radiation, while the read current after programming increases with the increase of the radiation doses as shown in Fig. 1(f). The read current and  $R_{OFF/ON}$  at -1.5 V read voltage as a function of total dose are shown in Fig. 1(g). The obvious increase of  $R_{OFF/ON}$  after 1 Mrad(Si) radiation can be clearly seen. This phenomenon can be explained by the change in the energy band caused by the TID radiation, shown in Figs. 1(d) and (f). Before radiation, programming causes positive polarization, which induces a band tilt in HZO and increases the F-N tunneling probability. Negative polarization has the opposite effect, reducing the F-N tunneling probability and read current. After radiation, the positive fixed charges increase the tunneling current of programmed devices, but after erasing, the probability of F-N tunneling is reduced, so those fixed charges have a negative effect on the erased read current. Figs. 1(h) and (i) show that  $\ln(I/V^2)$  is a function of  $1/V$  for the read current of programmed and erased states, respectively. In a high electric field,  $\ln(I/V^2)$  decreases linearly with  $(1/V)$ , indicating that the F-N tunneling is dominant. Moreover, at low electric field,  $\ln(I/V^2)$  increases at the logarithm of  $1/V$ , which is consistent with that of direct tunneling [3]. Hence, it can be seen that the F-N tunneling after programming is easier (Fig. 1(h)), while the F-N tunneling after erasing has no clear change with the increase in TID. This corresponds with our earlier analysis.

## References

- 1 Park M H, Kim H J, et al. Evolution of phases and ferroelectric properties of thin  $\text{Hf}_{0.5}\text{Zr}_{0.5}\text{O}_2$  films according to the thickness and annealing temperature. Appl Phys Lett, 2013, 102: 242905

\* Corresponding author (email: bijinshun@ime.ac.cn)

- 2 Shekhawat A, Walters G, et al. Data retention and low voltage operation of Al<sub>2</sub>O<sub>3</sub>/Hf<sub>0.5</sub>Zr<sub>0.5</sub>O<sub>2</sub> based ferroelectric tunnel junctions . *Nanotechnology*,2020, 31: 39LT01
- 3 Ryu H, Wu H, et al. Ferroelectric tunnel junctions based on aluminum oxide/ zirconium-doped hafnium oxide for neuromorphic computing . *Sci Rep*, 2019, 9: 20383

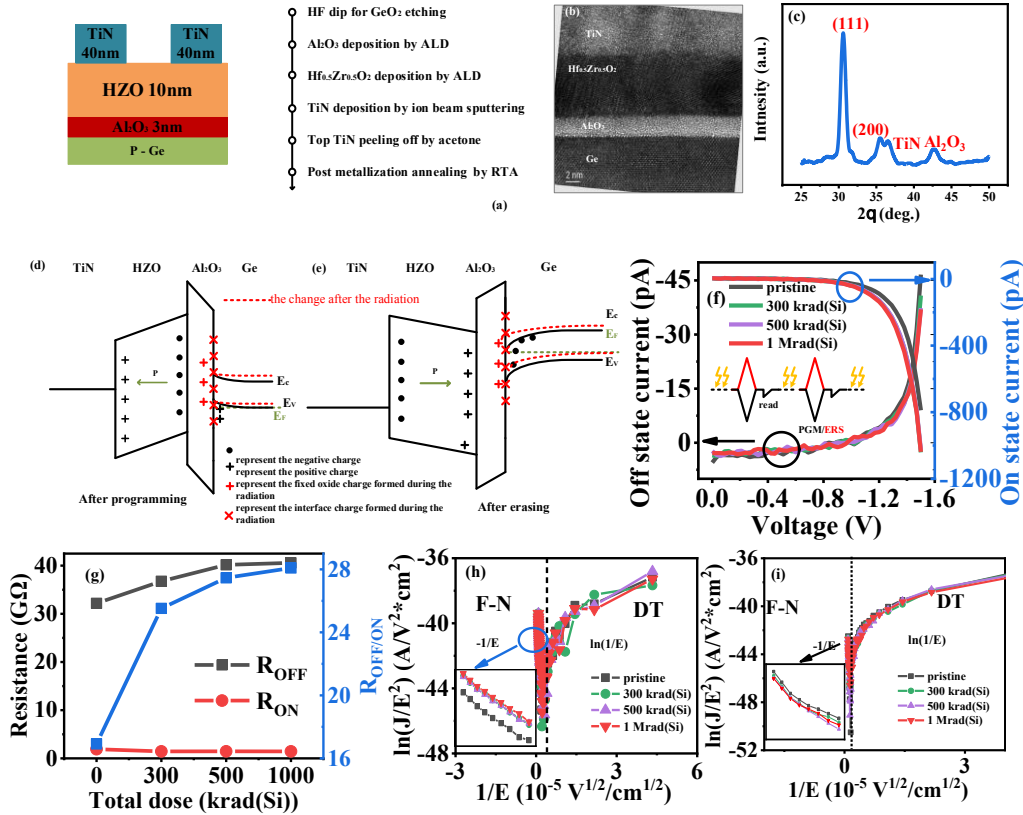


**Figure 1** (a) The illustration and fabrication flow of FTJs (not to scale); (b) the cross-sectional HRTEM image, and (c) the GIXRD spectrum of an FTJ device. (d) and (e) the energy energy diagrams of the programmed and erased FTJs before and after radiation; (f) The read currents as a function of voltage after  $-7.5$  V,  $10 \mu\text{s}$  programming (PGM) pulse and  $7.5$  V,  $10 \mu\text{s}$  erasing (ERS) pulse, the off/on state current are taken from the read dc IV sweep ( $-1.5$  V -  $0$  V), the inset shows the operation flow; The pulse trains are shown schematically in the insets; (g)  $R_{OFF/ON}$  at  $-1.5$  V after programming and erasing pulses as a function of TID and  $R_{OFF}$  and  $R_{ON}$  are the resistance values when the read voltage is  $-1.5$  V after erasing and programming, respectively; (h) and (i)  $\ln(I/V^2)$  as a function of  $1/V$  for the on and off state read current shown in (f), respectively.